



HAL
open science

A Fokker-Planck approach to the study of robustness in gene expression

Pierre Degond, Maxime Herda, Sepideh Mirrahimi

► **To cite this version:**

Pierre Degond, Maxime Herda, Sepideh Mirrahimi. A Fokker-Planck approach to the study of robustness in gene expression. *Mathematical Biosciences and Engineering*, 2020, 17 (6), pp.6459-6486. 10.3934/mbe.2020338 . hal-02882349v2

HAL Id: hal-02882349

<https://hal.science/hal-02882349v2>

Submitted on 14 Sep 2020

HAL is a multi-disciplinary open access archive for the deposit and dissemination of scientific research documents, whether they are published or not. The documents may come from teaching and research institutions in France or abroad, or from public or private research centers.

L'archive ouverte pluridisciplinaire **HAL**, est destinée au dépôt et à la diffusion de documents scientifiques de niveau recherche, publiés ou non, émanant des établissements d'enseignement et de recherche français ou étrangers, des laboratoires publics ou privés.

A FOKKER-PLANCK APPROACH TO THE STUDY OF ROBUSTNESS IN GENE EXPRESSION

P. DEGOND, M. HERDA, AND S. MIRRAHIMI

ABSTRACT. We study several Fokker-Planck equations arising from a stochastic chemical kinetic system modeling a gene regulatory network in biology. The densities solving the Fokker-Planck equations describe the joint distribution of the mRNA and μ RNA content in a cell. We provide theoretical and numerical evidence that the robustness of the gene expression is increased in the presence of μ RNA. At the mathematical level, increased robustness shows in a smaller coefficient of variation of the marginal density of the mRNA in the presence of μ RNA. These results follow from explicit formulas for solutions. Moreover, thanks to dimensional analyses and numerical simulations we provide qualitative insight into the role of each parameter in the model. As the increase of gene expression level comes from the underlying stochasticity in the models, we eventually discuss the choice of noise in our models and its influence on our results.

Keywords. Gene expression, microRNA, Fokker-Planck equations, Inverse Gamma distributions.

MSC 2020 Subject Classification. 35Q84, 92C40, 92D20, 35Q92, 65M08.

CONTENTS

1. Introduction	2
2. Presentation of the models	4
2.1. Dynamics of mRNA and μ RNA with binding	4
2.2. Dynamics of free mRNA without binding	5
2.3. Dynamics with binding and fast μ RNA	5
3. Well-posedness of the models and analytical formulas for solutions	6
3.1. Gamma and inverse gamma distributions	6
3.2. Explicit mRNA distribution without binding	7
3.3. Explicit mRNA distribution in the presence of fast μ RNA	8
3.4. Well-posedness of the main Fokker-Planck model	9
4. Noise reduction by binding : the case of fast μ RNA	10
4.1. Dimensional analysis	10
4.2. Cell to cell variation (CV)	11
4.3. Exploration of the parameter space	13
5. Noise reduction by binding for the main Fokker-Planck model: numerical evidence	14
5.1. Reformulation of the equation	14
5.2. Presentation of the numerical scheme	15
5.3. Numerical results	16
6. Comments on the choice of noise	16
6.1. Explicit formulas for distribution of mRNAs	18
6.2. Dimensional analysis	19
6.3. Numerical computation of the cell to cell variation	19
7. Concluding remarks and perspectives	20

Date: September 14, 2020.

Appendix A. Complementary results	21
A.1. Poincaré inequalities for gamma and inverse gamma distributions	21
A.2. An upper bound for the relative cell to cell variation	23
References	24

1. INTRODUCTION

This paper is concerned with a mathematical model for a gene regulatory network involved in the regulation of DNA transcription. DNA transcription is part of the mechanism by which a sequence of the nuclear DNA is translated into the corresponding protein. The transcription is initiated by the binding of a transcription factor, which is usually another protein, onto the gene's DNA-binding domain. Once bound, the transcription factor promotes the transcription of the nuclear DNA into a messenger RNA (further denoted by mRNA), which, once released, is translated into the corresponding protein by the ribosomes. This process is subject to a high level of noise due to the large variability of the conditions that prevail in the cell and the nucleus at the moment of the transcription. Yet, a rather stable amount of the final protein is needed for the good operation of the cell. The processes that regulate noise levels and maintain cell homeostasis have been scrutinized for a long time. Recently, micro RNAs (further referred to as μ RNAs) have occupied the front of the scene. These are very short RNAs which do not code for proteins. Many different sorts of μ RNAs are involved in various epigenetic processes. But one of their roles seems precisely the reduction of noise level in DNA transcription. In this scenario, the μ RNAs are synthesized together with the mRNAs. Then, some of the synthesized μ RNAs bind to the mRNAs and de-activate them. These μ RNA-bound mRNA become unavailable for protein synthesis. It has been proposed that this paradoxical mechanism which seems to reduce the efficiency of DNA transcription may indeed have a role in noise regulation (see [9, 19, 10] and the review [24]). The goal of the present contribution is to propose a mathematical model of the μ RNA-mRNA interaction and to use it to investigate the role of μ RNAs as potential noise regulators.

Specifically, in this paper, we propose a stochastic chemical kinetic model for the mRNA and μ RNA content in a cell. The production of mRNAs by the transcription factor and their inactivation through μ RNA binding are taken into account. More precisely, our model is a simplified version of the circuit used in [30, Fig. 2A and 2A']. We consider a ligand involved in the production of both an mRNA and a μ RNA, the μ RNA having the possibility to bind to the mRNA and deactivate it. By contrast to [30], we disregard the way the ligand is produced and consider that the ligand is such that there is a constant production rate of both mRNA and μ RNA. A second difference to [30] is that we disregard the transcription step of the mRNA into proteins. While [30] proposes to model the μ RNA as acting on translation, we assume that the μ RNA directly influences the number of mRNA available for transcription. Therefore, we directly relate the gene expression level to the number of μ RNA-free mRNA also referred to as the number of unbound mRNA. In order to model the stochastic variability in the production of the RNAs, a multiplicative noise is added to the production rate at all time. From the resulting system of stochastic differential equations, we introduce the joint probability density for mRNA and μ RNA which solves a deterministic Fokker-Planck equation. The mathematical object of interest is the stationary density solving the Fokker-Planck equation and more precisely the marginal density of the mRNA. The coefficient of variation (also called cell-to-cell variation) of this mRNA density, which is its

standard deviation divided by its the expectation, is often considered as the relevant criterion for measuring the robustness of gene expression (see for instance [30]).

Our main goal in this contribution is to provide theoretical and numerical evidence that the robustness of the gene expression is increased in the presence of μ RNA. At the theoretical level we derive a number of analytical formulas either for particular subsets of parameters of the model or under some time-scale separation hypotheses. From these formulas we can easily compute the cell to cell variation numerically and verify the increased robustness of gene expression when binding with μ RNA happens in the model. For general sets of parameters, the solution cannot be computed analytically. However we can prove well-posedness of the model and solve the PDE with a specifically designed numerical scheme. From the approximate solution, we compute the coefficient of variation and verify the hypothesis of increased gene expression.

Another classical approach to the study of noise in gene regulatory networks is through the chemical master equation [32] which is solved numerically by means of Gillespie's algorithm [21], see e.g. [13, 30]. Here, we use a stochastic chemical kinetic model through its associated Kolmogorov-Fokker-Planck equation. Chemical kinetics is a good approximation of the chemical master equation when the number of copies of each molecule is large. This is not the case in a cell where sometimes as few as a 100 copies of some molecules are available. Specifically, including a stochastic term in the chemical kinetic approach is a way to retain some of the randomness of the process while keeping the model complexity tractable. This ultimately leads to a Fokker-Planck model for the joint distribution of mRNAs and μ RNAs. In [18], a similar chemical kinetic model is introduced with a different modelling of stochasticity. The effect of the noise is taken into account by adding some uncertainty in the (steady) source term and the initial data. The authors are interested in looking at how this uncertainty propagates to the mRNA content and in comparing this uncertainty between situations including μ RNA production or not. The uncertainty is modeled by random variables with given probability density functions. Compared to [18], the Fokker-Planck approach has the advantage that the random perturbations do not only affect the initial condition and the source term, but are present at all times and vary through time. We believe that this is coherent with how stochasticity in a cell arises through time-varying ecological or biological factors.

While Fokker-Planck equations are widely used models in mathematical biology [31], their use for the study of gene regulatory network is, up to our knowledge, scarce (see e.g. [27]). Compared to other approaches, the Fokker-Planck model enables us to derive analytical formulas for solutions in certain cases. This is particularly handy for understanding the role of each parameter in the model, calibrating them from real-world data and perform fast numerical computations. Nevertheless, in the general case, the theoretical study and the numerical simulation of the model remains challenging because of the unboundedness of the drift and diffusion coefficients. We believe that we give below all the tools for handling these difficulties, and that our simple model provides a convincing mathematical interpretation of the increase of gene expression in the presence of μ RNAs.

The paper is organized as follows. In Section 2, we introduce the system of SDEs and the corresponding Fokker-Planck models. In Section 3, we discuss the well-posedness of the Fokker-Planck equations and derive analytical formulas for solutions under some simplifying hypotheses. In Section 4, we use the analytical formulas for solutions to give mathematical and numerical proofs of the decrease of cell-to-cell variation in the presence of μ RNA. In Section 5, we propose a numerical

scheme for solving the main Fokker-Planck model and gather further evidence confirming the hypothesis of increased gene expression from the simulations. Finally, in Section 6 we discuss the particular choice of multiplicative noise (*i.e.* the diffusion coefficient in the Fokker-Planck equation) in our model. In the appendix, we derive weighted Poincaré inequalities for gamma and inverse-gamma distributions which are useful in the analysis of Section 3. The code used for numerical simulations in this paper is publicly available on GitLab [17].

2. PRESENTATION OF THE MODELS

In this section, we introduce three steady Fokker-Planck models whose solutions describe the distribution of unbound mRNA and μ RNA within a cell. The solutions to these equations can be interpreted as the probability density functions associated with the steady states of stochastic chemical kinetic systems describing the production and destruction of mRNA and μ RNA. In Section 2.1 we introduce the main model for which the consumption of RNAs is either due to external factors in the cell (translation, *etc.*) or to binding between the two types of mRNA and μ RNA. Then, for comparison, in Section 2.2 we introduce the same model without binding between RNAs. Finally in Section 2.3, we derive an approximate version of the first model, by considering that reactions involving μ RNAs are infinitely faster than those involving mRNAs, which amplifies the binding phenomenon and mathematically allows for the derivation of analytical formulas for solutions. The latter will be made explicit in Section 3.

2.1. Dynamics of mRNA and μ RNA with binding. We denote by r_t the number of unbound mRNA and μ_t the number of unbound μ RNA of a given cell at time t . The kinetics of unbound mRNA and μ RNA is then given by the following stochastic differential equations

$$(1) \quad \begin{cases} dr_t &= (c_r - c r_t \mu_t - k_r r_t) dt + \sqrt{2\sigma_r} r_t dB_t^1, \\ d\mu_t &= (c_\mu - c r_t \mu_t - k_\mu \mu_t) dt + \sqrt{2\sigma_\mu} \mu_t dB_t^2, \end{cases}$$

with $c_r, c_\mu, k_r, k_\mu, \sigma_r, \sigma_\mu$ being some given positive constants and c being a given non-negative constant. Let us detail the meaning of each term in the modeling. The first term of each equation models the constant production of mRNA (*resp.* μ RNA) by the ligand at a rate c_r (*resp.* c_μ). The second term models the binding of the μ RNA to the mRNA. Unbound mRNA and μ RNA are consumed by this process at the same rate. The rate increases with both the number of mRNA and μ RNA. In the third term, the parameters k_r and k_μ are the rates of consumption of the unbound mRNA or μ RNA by various decay mechanisms. The last term in both equations represents stochastic fluctuations in the production and destruction mechanisms of each species. It relies on a white noise dB_t/dt where $B_t = (B_t^1, B_t^2)$ is a two-dimensional standard Brownian motion. The intensity of the stochastic noise is quantified by the parameters $\sqrt{2\sigma_r} r_t$ and $\sqrt{2\sigma_\mu} \mu_t$. Such a choice of multiplicative noise ensures that r_t and μ_t remain non-negative along the dynamics. The Brownian motions B_t^1 and B_t^2 are uncorrelated. The study of correlated noises or the introduction of extrinsic noise sources would be interesting, but will be discarded here.

In this paper we are interested in the invariant measure of (1) rather than the time dynamics described by the above SDEs. From the modelling point of view, we are considering a large number of identical cells and we assume that mRNA and μ RNA numbers evolve according to (1). Then we measure the distribution of both RNAs among the population, when it has reached a steady state $f \equiv f(r, \mu)$.

According to Itô's formula, the steady state should satisfy the following steady Fokker-Planck equation

$$(2) \quad \begin{cases} Lf(r, \mu) = 0, & (r, \mu) \in \Omega = (0, \infty)^2, \\ \int_{\Omega} f(r, \mu) dr d\mu = 1, & f(r, \mu) \geq 0. \end{cases}$$

where the Fokker-Planck operator is given by

$$(3) \quad Lf(r, \mu) := \partial_r [\partial_r(\sigma_r r^2 f) - (c_r - c r \mu - k_r r) f] + \partial_{\mu} [\partial_{\mu}(\sigma_{\mu} \mu^2 f) - (c_{\mu} - c r \mu - k_{\mu} \mu) f].$$

Since we do not model the protein production stage, we assume that the observed distribution of gene expression level is proportional to the marginal distribution of mRNA, *i.e.*

$$\rho(r) = \int_0^{\infty} f(r, \mu) d\mu.$$

By integration of (2) in the μ variable, ρ satisfies the equation

$$(4) \quad \partial_r [\partial_r(\sigma_r r^2 \rho) - (c_r - c r j_{\mu}(r) - k_r r) \rho] = 0.$$

The quantity $j_{\mu}(r)$ is the conditional expectation of the number of μ RNA within the population in the presence of r molecules of mRNA and it is given by

$$(5) \quad j_{\mu}(r) = \frac{1}{\rho(r)} \int \mu f(r, \mu) d\mu.$$

Before ending this paragraph, we note an alternate way to derive the Fokker-Planck equation (2) from the chemical master equation through the chemical Langevin equation. We refer the interested reader to [22].

2.2. Dynamics of free mRNA without binding. In the case where there is no μ RNA binding, namely when $c = 0$, the variables r and μ are independent. Thus, the densities of the invariant measures satisfying (2) are of the form

$$f_0(r, \mu) = \rho_0(r) \lambda(\mu),$$

where $\lambda(\mu)$ is the density of the marginal distribution of μ RNA. From the modelling point of view, it corresponds to the case where there is no feed-forward loop from μ RNA. Therefore, only the dynamics on mRNA, and thus ρ_0 , is of interest in our study. It satisfies the following steady Fokker-Planck equation obtained directly from (4),

$$(6) \quad \begin{cases} \partial_r [\sigma_r \partial_r(r^2 \rho_0) - (c_r - k_r r) \rho_0] = 0, \\ \int_0^{\infty} \rho_0(r) dr = 1, & \rho_0(r) \geq 0. \end{cases}$$

It can be solved explicitly as we will discuss in Section 3.2.

2.3. Dynamics with binding and fast μ RNA. The Fokker-Planck equation (2) cannot be solved explicitly. However, one can make some additional assumptions in order to get an explicit invariant measure providing some insight into the influence of the binding mechanism with μ RNA. This is the purpose of the model considered hereafter.

Let us assume the μ RNA-mRNA binding rate, the μ RNA decay and the noise on μ RNA are large. Since the sink term of the μ RNA equation is large, it is also

natural to assume that the μ RNA content is small. Mathematically, we assume the following scaling

$$c = \frac{\tilde{c}}{\varepsilon}, \quad k_\mu = \frac{\tilde{k}_\mu}{\varepsilon}, \quad \sigma_\mu = \frac{\tilde{\sigma}_\mu}{\varepsilon}, \quad \mu_t = \varepsilon \tilde{\mu}_t,$$

for some small constant $\varepsilon > 0$. Then $(r_t, \tilde{\mu}_t)$ satisfies

$$\begin{cases} dr_t &= (c_r - \tilde{c} r_t \tilde{\mu}_t - \tilde{k}_r r_t) dt + \sqrt{2\sigma_r} r_t dB_t^1, \\ \varepsilon d\tilde{\mu}_t &= (c_\mu - \tilde{c} r_t \tilde{\mu}_t - \tilde{k}_\mu \tilde{\mu}_t) dt + \sqrt{2\varepsilon\tilde{\sigma}_\mu} \tilde{\mu}_t dB_t^2, \end{cases}$$

whose corresponding steady Fokker-Planck equation for the invariant measure then writes, dropping the tilde,

$$\begin{aligned} \partial_r [\partial_r (\sigma_r r^2 f_\varepsilon) - (c_r - c r \mu - k_r r) f_\varepsilon] \\ + \frac{1}{\varepsilon} \partial_\mu [\partial_\mu (\sigma_\mu \mu^2 f_\varepsilon) - (c_\mu - c r \mu - k_\mu \mu) f_\varepsilon] = 0 \end{aligned}$$

In the limit case where $\varepsilon \rightarrow 0$, one may expect that at least formally, the density f_ε converges to a limit density f_{fast} satisfying

$$\partial_\mu [\partial_\mu (\sigma_\mu \mu^2 f_{\text{fast}}) - (c_\mu - c r \mu - k_\mu \mu) f_{\text{fast}}] = 0.$$

As r is only a parameter in the previous equation and since the first marginal of f_ε still satisfies (4) for all ε , one should have (formally)

$$(7) \quad \begin{cases} f_{\text{fast}}(r, \mu) = \rho_{\text{fast}}(r) M(r, \mu) \geq 0, \\ \partial_\mu [\partial_\mu (\sigma_\mu \mu^2 M) - (c_\mu - c r \mu - k_\mu \mu) M] = 0, \\ \partial_r [\partial_r (\sigma_r r^2 \rho_{\text{fast}}) - (c_r - c r j_{\text{fast}}(r) - k_r r) \rho_{\text{fast}}] = 0, \\ \int_0^\infty \rho_{\text{fast}}(r) dr = 1, \quad \int_0^\infty M(r, \mu) d\mu = 1, \\ j_{\text{fast}}(r) = \int_0^\infty \mu M(r, \mu) d\mu. \end{cases}$$

3. WELL-POSEDNESS OF THE MODELS AND ANALYTICAL FORMULAS FOR SOLUTIONS

In this section, we show that the three previous models are well-posed. For the Fokker-Planck equations (6) and (7), we explicitly compute the solutions. They involve inverse gamma distributions.

3.1. Gamma and inverse gamma distributions. The expressions of the gamma and inverse gamma probability densities are respectively

$$(8) \quad \gamma_{\alpha, \beta}(x) = C_{\alpha, \beta} x^{\alpha-1} \exp(-\beta x),$$

and

$$(9) \quad g_{\alpha, \beta}(y) = \frac{C_{\alpha, \beta}}{y^{1+\alpha}} \exp\left(-\frac{\beta}{y}\right),$$

for $x, y \in (0, \infty)$. The normalization constant is given by $C_{\alpha, \beta} = \beta^\alpha / \Gamma(\alpha)$ where Γ is the Gamma function. Observe that by the change of variable $y = 1/x$ one has

$$g_{\alpha, \beta}(y) dy = \gamma_{\alpha, \beta}(x) dx$$

which justifies the terminology. Let us also recall that the first and second moments of the inverse gamma distribution are

$$(10) \quad \int_0^\infty y g_{\alpha, \beta}(y) dy = \frac{\beta}{\alpha-1}, \quad \text{if } \alpha > 1, \beta > 0,$$

$$(11) \quad \int_0^\infty y^2 g_{\alpha,\beta}(y) dy = \frac{\beta^2}{(\alpha-1)(\alpha-2)}, \quad \text{if } \alpha > 2, \beta > 0,$$

Interestingly enough, we can show (see Appendix A.1 for details and additional results) that inverse gamma distributions with finite first moment ($\alpha > 1$) satisfy a (weighted) Poincaré inequality. The proof of the following proposition is done in Appendix A.1 among more general considerations.

Proposition 3.1. *Let $\alpha > 1$ and $\beta > 0$. Then, for any function v such that the integrals make sense, one has*

$$(12) \quad \int_0^\infty |v(y) - \langle v \rangle_{g_{\alpha,\beta}}|^2 g_{\alpha,\beta}(y) dy \leq \frac{1}{\alpha-1} \int_0^\infty |v'(y)|^2 g_{\alpha,\beta}(y) y^2 dy,$$

where for any probability density ν and any function u on $(0, \infty)$, the notation $\langle u \rangle_\nu$ denotes $\int u \nu$.

3.2. Explicit mRNA distribution without binding. In the case of free mRNAs, a solution to (6) can be computed explicitly and takes the form of an inverse gamma distribution.

Lemma 3.2. *The following inverse gamma distribution*

$$(13) \quad \rho_0(r) = g_{1+\frac{k_r}{\sigma_r}, \frac{c_r}{\sigma_r}}(r) = C_{1+\frac{k_r}{\sigma_r}, \frac{c_r}{\sigma_r}} \frac{1}{r^{2+\frac{k_r}{\sigma_r}}} \exp\left(-\frac{c_r}{\sigma_r r}\right)$$

is the only classical solution to (6).

Proof. First observe that

$$\partial_r [\sigma_r \partial_r (r^2 \rho_0) - (c_r - k_r r) \rho_0] = \partial_r \left[\sigma_r r^2 g_{1+\frac{k_r}{\sigma_r}, \frac{c_r}{\sigma_r}} \partial_r \left(\rho_0 g_{1+\frac{k_r}{\sigma_r}, \frac{c_r}{\sigma_r}}^{-1} \right) \right].$$

Therefore a solution of (8) must be of the form

$$\rho_0(r) = C_1 g_{1+\frac{k_r}{\sigma_r}, \frac{c_r}{\sigma_r}} \int_1^r \sigma_r^{-1} r^{-2} g_{1+\frac{k_r}{\sigma_r}, \frac{c_r}{\sigma_r}}^{-1}(r) dr + C_2 g_{1+\frac{k_r}{\sigma_r}, \frac{c_r}{\sigma_r}},$$

for some constants C_1, C_2 . The first term decays like $1/r$ at infinity, thus the only probability density ρ_0 of this form is obtained for $C_1 = 0$ and $C_2 = 1$. \square

The Poincaré inequality (12) tells us that the solution of Lemma 3.2 is also the only (variational) solution in the appropriate weighted Sobolev space. Indeed, we may introduce the natural Hilbert space associated with Equation (6),

$$X_{\alpha,\beta} = \{v : (0, \infty) \rightarrow \mathbb{R}, \|v\|_{X_{\alpha,\beta}} < \infty\}$$

with a squared norm given by

$$\|v\|_{X_{\alpha,\beta}}^2 = \int_0^\infty \left([(v/g_{\alpha,\beta})(y)]^2 + [(v/g_{\alpha,\beta})'(y)]^2 y^2 \right) g_{\alpha,\beta}(y) dy.$$

Then the following uniqueness result holds.

Lemma 3.3. *The classical solution $\rho_0 = g_{1+\frac{k_r}{\sigma_r}, \frac{c_r}{\sigma_r}}$ is the only solution of (6) in $X_{1+\frac{k_r}{\sigma_r}, \frac{c_r}{\sigma_r}}$.*

Proof. If ρ_0 and $\tilde{\rho}_0$ are two solutions of (6), a straightforward consequence of (12) is that $\|\rho_0 - \tilde{\rho}_0\|_{X_{1+\frac{k_r}{\sigma_r}, \frac{c_r}{\sigma_r}}} = 0$. This is obtained by integrating the difference between the equation on ρ_0 and $\tilde{\rho}_0$ against $(\rho_0 - \tilde{\rho}_0) g_{1+\frac{k_r}{\sigma_r}, \frac{c_r}{\sigma_r}}^{-1}$. \square

Another consequence of the Poincaré inequality is that if we consider the time evolution associated with the equation (6) then solutions converge exponentially fast towards the steady state ρ_0 . This justifies our focus on the stationary equations. The transient regime is very short and equilibrium is reached quickly. We can quantify the rate of convergence in terms of the parameters.

Proposition 3.4. *Let ξ solve the Fokker-Planck equation*

$$\partial_t \xi(t, r) = \partial_r \left[\sigma_r \partial_r (r^2 \xi(t, r)) - (c_r - k_r r) \xi(t, r) \right],$$

starting from the probability density $\xi(0, r, \mu) = \xi^{in}(r, \mu)$. Then for all $t \geq 0$,

$$\begin{aligned} \int_0^\infty (\xi(t, r) - \rho_0(r))^2 g_{1+\frac{k_r}{\sigma_r}, \frac{c_r}{\sigma_r}}^{-1}(r) dr \\ \leq e^{-\frac{k_r}{\sigma_r} t} \int_0^\infty (\xi^{in}(r) - \rho_0(r))^2 g_{1+\frac{k_r}{\sigma_r}, \frac{c_r}{\sigma_r}}^{-1}(r) dr. \end{aligned}$$

Proof. Observe that $\xi - \rho_0$ solves the unsteady Fokker-Planck equation, so that by multiplying the equation by $(\xi - \rho_0) g_{1+\frac{k_r}{\sigma_r}, \frac{c_r}{\sigma_r}}^{-1}$ and integrating in r one gets

$$\begin{aligned} \frac{d}{dt} \int_0^\infty (\xi(t, r) - \rho_0(r))^2 g_{1+\frac{k_r}{\sigma_r}, \frac{c_r}{\sigma_r}}^{-1}(r) dr \\ + \int_0^\infty \left| \partial_r \left(\frac{\xi(t, \cdot) - \rho_0}{g_{1+\frac{k_r}{\sigma_r}, \frac{c_r}{\sigma_r}}} \right) (r) \right|^2 g_{1+\frac{k_r}{\sigma_r}, \frac{c_r}{\sigma_r}}(r) r^2 dr = 0. \end{aligned}$$

Then by using the Poincaré inequality (12) and a Gronwall type argument, one gets the result. \square

3.3. Explicit mRNA distribution in the presence of fast μ RNA. Now we focus on the solution of (7). The same arguments as those establishing Lemma 3.3 show that the only function M satisfying (7) is the following inverse gamma distribution

$$(14) \quad M(r, \mu) = g_{1+\frac{k_\mu}{\sigma_\mu} + \frac{c}{\sigma_\mu} r, \frac{c_\mu}{\sigma_\mu}}(\mu).$$

Then an application of (10) yields

$$(15) \quad j_{\text{fast}}(r) = \frac{c_\mu}{k_\mu + cr}.$$

It remains to find ρ_{fast} which is a probability density solving the Fokker-Planck equation

$$\partial_r \left[\partial_r (\sigma_r r^2 \rho_{\text{fast}}) - \left(c_r - \frac{c_\mu cr}{k_\mu + cr} - k_r r \right) \rho_{\text{fast}} \right] = 0.$$

Arguing as in the proof of Lemma 3.2, one observe that integrability properties force ρ_{fast} to actually solve

$$\partial_r (\sigma_r r^2 \rho_{\text{fast}}) - \left(c_r - \frac{c_\mu cr}{k_\mu + cr} - k_r r \right) \rho_{\text{fast}} = 0.$$

which yields

$$(16) \quad \rho_{\text{fast}}(r) = C \left(1 + \frac{k_\mu}{cr} \right)^{\frac{c c_\mu}{\sigma_r k_\mu}} \frac{1}{r^{2+\frac{k_r}{\sigma_r}}} \exp \left(-\frac{c_r}{\sigma_r r} \right)$$

where $C \equiv C(c_r, c_\mu, k_r, k_\mu, \sigma_r, \sigma_\mu, c)$ is a normalizing constant making ρ_{fast} a probability density function.

3.4. Well-posedness of the main Fokker-Planck model. Now we are interested in the well-posedness of (2), for which we cannot derive explicit formulas anymore. Despite the convenient functional framework introduced in Section 3.2, classical arguments from elliptic partial differential equation theory do not seem to be adaptable to the case $c > 0$. The main obstruction comes from an incompatibility between the natural decay of functions in the space $X_{\alpha,\beta}$ and the rapid growth of the term $c r \mu$ when $|(r, \mu)| \rightarrow \infty$.

However, thanks to the results of [26] focused specifically on Fokker-Planck equations, we are able to prove well-posedness of the steady Fokker-Planck equation (2). The method is based on finding a Lyapunov function for the adjoint of the Fokker-Planck operator and relies on an integral identity proved by the same authors in [25]. The interested reader may also find additional material and a comprehensive exposition concerning the analysis of general Fokker-Planck equations for measures in [12].

First of all let us specify the notion of solution. A weak solution to (2) is an integrable function f such that

$$(17) \quad \begin{cases} \int_{\Omega} f(r, \mu) \mathcal{L}\varphi(r, \mu) = 0, & \text{for all } \varphi \in \mathcal{C}_c^\infty(\Omega), \\ \int_{\Omega} f(r, \mu) = 1, & f(r, \mu) \geq 0, \end{cases}$$

where the adjoint operator is given by

$$(18) \quad \mathcal{L}\varphi(r, \mu) := \sigma_r r^2 \partial_{rr}^2 \varphi + (c_r - c r \mu - k_r r) \partial_r \varphi \\ + \sigma_\mu \mu^2 \partial_{\mu\mu}^2 \varphi + (c_\mu - c r \mu - k_\mu \mu) \partial_\mu \varphi.$$

A reformulation and combination of [26, Theorem A and Proposition 2.1] provides the following result.

Proposition 3.5 ([26]). *Assume that there is a smooth function $U : \Omega \rightarrow [0, +\infty)$, called Lyapunov function with respect to \mathcal{L} , such that*

$$(19) \quad \lim_{(r,\mu) \rightarrow \partial\bar{\Omega}} U(r, \mu) = +\infty,$$

and

$$(20) \quad \lim_{(r,\mu) \rightarrow \partial\bar{\Omega}} \mathcal{L}U(r, \mu) = -\infty,$$

where $\partial\bar{\Omega} = \partial\Omega \cup (\{+\infty\} \times \mathbb{R}_+) \cup (\mathbb{R}_+ \times \{+\infty\})$. Then there is a unique f satisfying (17). Moreover $f \in W_{\text{loc}}^{1,\infty}(\Omega)$.

Remark 3.6. *The method of Lyapunov functions is a standard tool for proving well-posedness of many problems in the theory of ordinary differential equations, dynamical systems... For diffusion processes and Fokker-Planck equations its use dates back to Has'minskii [23]. We refer to [12, Chapter 2], [26] and references therein for further comments on the topic. Let us stress however that Lyapunov functions are not related (at least directly) to the Lyapunov (or entropy) method for evolution PDEs in which one shows the monotony of a functional to quantify long-time behavior.*

Remark 3.7. *Thanks of the degeneracy of the diffusivities at $r = 0$ and $\mu = 0$ and the Lyapunov function condition, one doesn't need supplementary boundary conditions in (17) for the problem to have a unique solution. This is different from standard elliptic theory where boundary conditions are necessary to define a unique solution when the domain and the coefficients are bounded with uniformly elliptic diffusivities. Further comments may be found in [26].*

Lemma 3.8. *Choose any two constants $b_r > \frac{c}{k_\mu}$ and $b_\mu > \frac{c}{k_r}$. Then, the function $U : \Omega \rightarrow \mathbb{R}$ defined by*

$$U(r, \mu) = b_r r - \ln(b_r r) + b_\mu \mu - \ln(b_\mu \mu)$$

is a Lyapunov function with respect to \mathcal{L} (i.e. it is positive on Ω and it satisfies (19) and (20)).

Proof. First observe that condition (19) is clearly satisfied. Also, U is minimal at (b_r^{-1}, b_μ^{-1}) where it takes the value 2 and thus it is positive on Ω . Finally a direct computation yields

$$\begin{aligned} \mathcal{L}U(r, \mu) &= (\sigma_r + \sigma_\mu + b_r c_r + b_\mu c_\mu + k_r + k_\mu) \\ &\quad - \frac{c_r}{r} - \frac{c_\mu}{\mu} - (b_r k_r - c)r - (b_\mu k_\mu - c)\mu - cr\mu(b_r + b_\mu), \end{aligned}$$

and (20) follows. \square

Now we state our well-posedness result for the Fokker-Planck equation (17).

Proposition 3.9. *There is a unique weak solution f to the steady Fokker-Planck equation (2). Moreover, f is indefinitely differentiable in Ω .*

Proof. The existence and uniqueness of a solution $f \in W_{\text{loc}}^{1,\infty}(\Omega)$ is a combination of Proposition 3.5 and Lemma 3.8. From there in any smooth compact subdomain $K \subset\subset \Omega$, we get from standard elliptic theory [20] that $f \in \mathcal{C}^\infty(K)$, since the coefficients are smooth and the operator is uniformly elliptic. \square

4. NOISE REDUCTION BY BINDING : THE CASE OF FAST μ RNA

In this section we focus on the comparison between the explicit distributions (13) and (16). We are providing theoretical and numerical evidence that the coefficient of variation (which is a normalized standard deviation) of (16) is less than that of (13). This quantity called cell to cell variation in the biological literature [30] characterizes the robustness of the gene expression level (the lower the better). We start by performing a rescaling in order to extract the dimensionless parameters which characterize the distributions.

4.1. Dimensional analysis. In order to identify the parameters of importance in the models, we rescale the variables r and μ around characteristic values \bar{r} and $\bar{\mu}$ chosen to be

$$(21) \quad \bar{r} = \frac{c_r}{k_r} \quad \text{and} \quad \bar{\mu} = \frac{c_\mu}{k_\mu}.$$

These choices are natural in the sense that they correspond to the steady states of the mRNA and μ RNA dynamics without binding nor stochastic effects, that is respectively $dr_t = (c_r - k_r r_t) dt$ and $d\mu_t = (c_\mu - k_\mu \mu_t) dt$. When the noise term is added, it still corresponds to the expectation of the invariant distribution, that is the first moment of ρ_0 in the case of mRNA. We introduce f^{ad} such that for all $(r, \mu) \in \Omega$ one has

$$\frac{1}{\bar{r}\bar{\mu}} f^{\text{ad}}\left(\frac{r}{\bar{r}}, \frac{\mu}{\bar{\mu}}\right) = f(r, \mu).$$

After some computations one obtains that the Fokker-Planck equation (2)-(3) can be rewritten in terms of f^{ad} as

$$(22) \quad \begin{aligned} \partial_r [\delta(1 - \gamma p r \mu - r) f^{\text{ad}} - \partial_r (r^2 f^{\text{ad}})] \\ + \partial_\mu [\delta \kappa (1 - \gamma r \mu - \mu) f^{\text{ad}} - \nu \partial_\mu (\mu^2 f^{\text{ad}})] = 0, \end{aligned}$$

The marginal distributions ρ_0 and ρ_{fast} are rescaled into dimensionless densities

$$(23) \quad \rho_0^\delta(r) = g_{1+\delta,\delta}(r) = C_0^{\text{ad}} \frac{1}{r^{2+\delta}} \exp\left(-\frac{\delta}{r}\right)$$

$$(24) \quad \rho_{\text{fast}}^{\delta,\gamma,p}(r) = C_{\text{fast}}^{\text{ad}} \left(1 + \frac{1}{\gamma r}\right)^{\gamma p \delta} \frac{1}{r^{2+\delta}} \exp\left(-\frac{\delta}{r}\right)$$

where C_0^{ad} and $C_{\text{fast}}^{\text{ad}}$ are normalizing constants depending on the parameters of the model and δ , p and γ are dimensionless parameters. The first parameter

$$(25) \quad \delta = \frac{k_r}{\sigma_r},$$

only depends on constants that are independent of the dynamics of μ RNAs. The two other dimensionless parameters appearing in the marginal distribution of mRNA in the presence of fast μ RNA are

$$(26) \quad p = \frac{c_\mu}{c_r},$$

and

$$(27) \quad \gamma = \frac{c\bar{r}}{k_\mu} = \frac{c c_r}{k_\mu k_r}.$$

Let us give some insight into the biological meaning of these parameters. The parameter γ measures the relative importance of the two mechanisms of destruction of μ RNAs, namely the binding with mRNAs versus the natural destruction/consumption. A large γ means that the binding effect is strong and conversely. The parameter p compares the production rate of μ RNAs with that of mRNAs. Large values of p mean that there are much more μ RNAs than mRNAs produced per unit of time.

Finally, in the Fokker-Planck model (22), there are also two other parameters which are

$$(28) \quad \kappa = \frac{k_\mu}{k_r},$$

and

$$(29) \quad \nu = \frac{\sigma_\mu}{\sigma_r}.$$

The parameter κ compares consumption of μ RNA versus that of mRNA by mechanisms which are not the binding between the two RNAs. The parameter ν compares the amplitude of the noise in the dynamics of μ RNA versus that of the mRNA.

Remark 4.1. *Observe that the approximation of fast μ RNA leading to the model discussed in Section 2.3 in its dimensionless form amounts to taking $\nu = \kappa = 1/\varepsilon$ and letting ε tend to 0.*

4.2. Cell to cell variation (CV). For any suitably integrable non-negative function ν , let us denote by

$$m_k(\nu) = \int y^k \nu(y) dy$$

its k -th moment. The coefficient of variation or cell to cell variation (CV) is defined by

$$(30) \quad \text{CV}(\nu) = \frac{\text{Var}(\nu/m_0(\nu))^{1/2}}{\text{Exp}(\nu/m_0(\nu))} = \left(\frac{m_2(\nu)m_0(\nu)}{m_1(\nu)^2} - 1 \right)^{1/2}$$

where $\text{Exp}(\cdot)$ and $\text{Var}(\cdot)$ denote the expectation and variance. Let us state a first lemma concerning some cases where the coefficient of variation can be computed exactly.

Lemma 4.2. *Consider the dimensionless distributions defined in (23) and (24). Then one has that*

$$(31) \quad \text{Exp}(\rho_0^\delta) = 1, \quad \text{Var}(\rho_0^\delta) = \frac{1}{\delta - 1}, \quad \text{CV}(\rho_0^\delta) = \frac{1}{\sqrt{\delta - 1}},$$

where the variance and coefficient of variation are well-defined only for $\delta > 1$. Then for any $\delta > 1$, the following limits holds

$$\begin{aligned} \lim_{\gamma \rightarrow 0} \text{CV}(\rho_{fast}^{\delta, \gamma, p}) &= \text{CV}(\rho_0^\delta), \quad \forall p > 0, \\ \lim_{p \rightarrow 0} \text{CV}(\rho_{fast}^{\delta, \gamma, p}) &= \text{CV}(\rho_0^\delta), \quad \forall \gamma > 0, \\ \lim_{\gamma \rightarrow \infty} \text{CV}(\rho_{fast}^{\delta, \gamma, p}) &= \text{CV}(\rho_0^\delta), \quad \forall p \in [0, 1]. \end{aligned}$$

Proof. The formulas for the moments follow from (10) and (11). Then observe that for all r , one has

$$\lim_{\gamma \rightarrow 0} \rho_{fast}^{\delta, \gamma, p}(r) = \lim_{p \rightarrow 0} \rho_{fast}^{\delta, \gamma, p}(r) = \rho_0^\delta(r)$$

and

$$\lim_{\gamma \rightarrow +\infty} \rho_{fast}^{\delta, \gamma, p}(r) = g_{1+\delta, (1-p)\delta}(r)$$

and one can then take limits in integrals by dominated convergence. \square

Let us give a biological interpretation of the previous lemma. When $\gamma = 0$ or $p = 0$, which respectively corresponds to the cases where there is no binding between mRNA and μ RNA or there is no production of μ RNA, the coefficient of variation is unchanged from the case of free mRNAs. The last limit states that if the μ RNA production is weaker than the mRNA production, then in the regime where all μ RNA is consumed by binding with mRNA, the coefficient of variation is also unchanged.

Outside of these asymptotic regimes, the theoretical result one would like to have is the following.

Conjecture 4.3. *For any $\delta > 1$, $\gamma, p > 0$ and one has $\text{CV}(\rho_{fast}^{\delta, \gamma, p}) \leq \text{CV}(\rho_0^\delta)$.*

At the moment, we are able to obtain the following uniform in γ and p bound

$$(32) \quad \text{CV}(\rho_{fast}^{\delta, \gamma, p}) \leq C_\delta := \left(\left(\frac{\delta}{\delta - 1} \right)^2 \left(1 - \frac{1}{(\delta - 1)^2} \right)^{\delta - 2} - 1 \right)^{\frac{1}{2}},$$

which holds for all $\delta > 2$, $\gamma > 0$ and $p \geq 0$. The result is proved in Proposition A.6 in the Appendix. Observe that $C_\delta \geq \text{CV}(\rho_0^\delta)$ but asymptotically

$$C_\delta \sim_{\delta \rightarrow \infty} \text{CV}(\rho_0^\delta) = \frac{1}{\sqrt{\delta - 1}},$$

so that C_δ is fairly close to $\text{CV}(\rho_0^\delta)$ for large δ . In the next section we provide numerical evidence that it should be possible to improve the right-hand side of (32) and prove Conjecture 4.3. Let us also mention that using integration by parts formulas it is possible to establish a recurrence relation between moments. From there one can infer the inequality of Conjecture 4.3 for subsets of parameters (γ, p) . As the limitation to these subsets is purely technical and do not have any particular biological interpretation we do not report these results here.

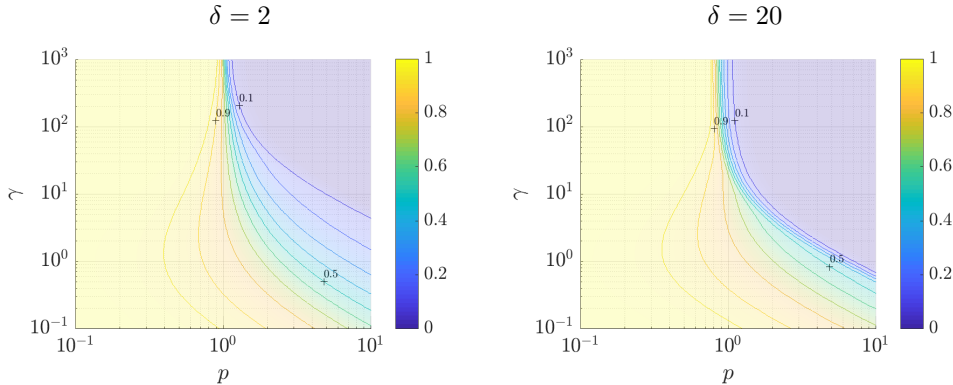


FIGURE 1. **Exploration of the parameter space.** Relative cell to cell variation $CV(\rho_{\text{fast}}^{\delta,\gamma,p})/CV(\rho_0^\delta)$ for various parameters p , γ and δ . On the horizontal axis, left means more production of mRNA and right means more production of μ RNA; On the vertical axis, top means more destruction of mRNA by binding and bottom means more destruction/consumption of mRNA by other mechanisms

4.3. Exploration of the parameter space. Now, we explore the space of parameters (δ, γ, p) in order to compare the cell to cell variation in the case of fast μ RNA and in the case of free mRNA.

In order to evaluate numerically the cell to cell variation we need to compute $m_k(\rho_{\text{fast}}^{\delta,\gamma,p})$, for $k = 0, 1, 2$. Observe that after a change of variable these quantities can be rewritten (up to an explicit multiplicative constant depending on parameters)

$$I_k = \int_0^\infty f_k(s) s^{\delta-2} e^{-s} ds,$$

with $f_k(s) = s^{2-k}(1+s/(\gamma\delta))^{p\gamma\delta}$. For the numerical computation of these integrals, we use a Gauss-Laguerre quadrature

$$I_k \approx \sum_{i=1}^N \omega_i^N f_k(x_i^N).$$

which is natural and efficient as we are dealing with functions integrated against a gamma distribution. We refer to [29] and references therein for the definition of the coefficients ω_i^N and quadrature points x_i^N . The truncation order N is chosen such that the numerical error between the approximation at order N and $N+1$ is inferior to the given precision 10^{-8} when $p \leq 1$. For $p \geq 1$, the function f_k may take large values and it is harder to get the same numerical precision. In the numerical results below the mean error for the chosen sets of parameters with large values of p is around 10^{-4} and the maximal error is 10^{-2} . This is good enough to comment on qualitative behavior. The code used for these numerical simulations is publicly available on GitLab [17].

We plot the relative cell to cell variation $CV(\rho_{\text{fast}}^{\delta,\gamma,p})/CV(\rho_0^\delta)$ with respect to γ and p for two different values of δ . The results are displayed on Figure 1. Then, on Figure 2, we draw the explicit distributions $\rho_{\text{fast}}^{\delta,\gamma,p}$ for various sets of parameters and compare it with ρ_0^δ .

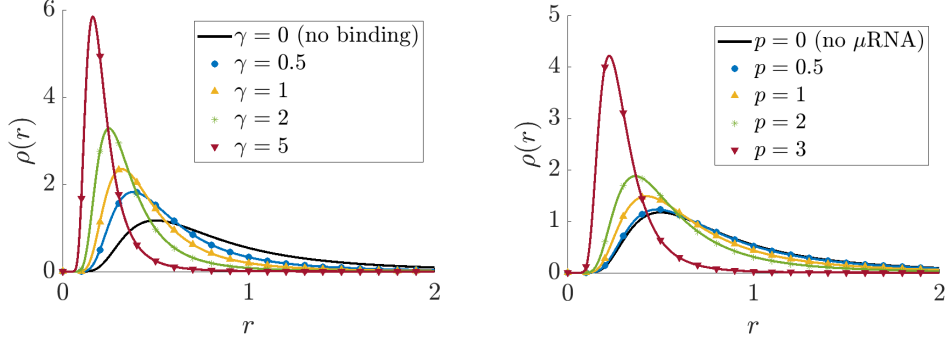


FIGURE 2. Marginal distributions of mRNAs $\rho_{\text{fast}}^{\delta, \gamma, p}$ for fast μ RNAs compared to the free mRNA distribution ρ_0^δ (black solid curve) for different parameters p and γ . Left: $\delta = 2$, $p = 1.5$ and γ varies. Right: $\delta = 2$, $\gamma = 1$ and p varies.

The numerical simulations of Figure 1 suggest that the bound (32) is non-optimal and Conjecture 4.3 should be satisfied. Observe also that the asymptotics of Lemma 4.2 are illustrated.

From a modeling point of view, these simulations confirm that for any choice of parameter, the presence of (fast) μ RNA makes the cell to cell variation decrease compared to the case without μ RNA. Moreover, the qualitative behavior with respect to the parameters makes sense. Indeed we observe that whenever enough μ RNA is produced ($p \geq 1$), the increase of the binding phenomenon ($\gamma \rightarrow \infty$) makes the cell to cell variation decay drastically.

5. NOISE REDUCTION BY BINDING FOR THE MAIN FOKKER-PLANCK MODEL: NUMERICAL EVIDENCE

In this section, we compute the gene expression level of the main model described by equation (2). In this case, as there is no explicit formula for the solution, we will compute an approximation of it using a discretization of the Fokker-Planck equation. In order to compute the solution in practice, we restrict the domain to the bounded domain $\Omega_b = [r_{\min}, r_{\max}] \times [\mu_{\min}, \mu_{\max}]$. Because of the truncation, we add zero-flux boundary conditions in order to keep a conservative equation. It leads to the problem

$$(33) \quad \begin{cases} \partial_r [(c_r - c r \mu - k_r r) f - \partial_r (\sigma_r r^2 f)] \\ \quad + \partial_\mu [(c_\mu - c r \mu - k_\mu \mu) f - \partial_\mu (\sigma_\mu \mu^2 f)] = 0, & \text{in } \Omega_b \\ \partial_r (\sigma_r r^2 f) - (c_r - c r \mu - k_r r) f = 0, & \text{if } r = r_{\min} \text{ or } r_{\max}, \\ \partial_\mu (\sigma_\mu \mu^2 f) - (c_\mu - c r \mu - k_\mu \mu) f = 0, & \text{if } \mu = \mu_{\min} \text{ or } \mu_{\max}, \\ \int_{\Omega_b} f \, dr \, d\mu = 1. \end{cases}$$

5.1. Reformulation of the equation. In order for the numerical scheme to be more robust with respect to the size of the parameters, we discretize the equation in dimensionless version (22). It will also allow for comparisons with numerical experiments of the previous sections.

As the coefficients in the advection and diffusion parts of (22) grow rapidly in r , μ and degenerate when $r = 0$ and $\mu = 0$, the design of an efficient numerical solver for (22) is not straightforward. Moreover a desirable feature of the scheme would be

a preservation of the analytically known solution corresponding to $\gamma = 0$. Because of these considerations we will discretize a reformulated version of the equation in which the underlying inverse gamma distributions explicitly appear. It will allow for a better numerical approximation when r and μ are either close to 0 or large. The reformulation is the following

$$(34) \quad -\partial_r \left[r^2 h^{(1)}(r, \mu) \partial_r \left(\frac{f^{\text{ad}}}{h^{(1)}(r, \mu)} \right) \right] - \partial_\mu \left[\nu \mu^2 h^{(2)}(r, \mu) \partial_\mu \left(\frac{f^{\text{ad}}}{h^{(2)}(r, \mu)} \right) \right] = 0,$$

with the associated no-flux boundary conditions and where the functions $h^{(1)}$ and $h^{(2)}$ are given by

$$(35) \quad h^{(1)}(r, \mu) = r^{-(1+p\mu\gamma)\delta-2} \exp\left(-\frac{\delta}{r}\right),$$

and

$$(36) \quad h^{(2)}(r, \mu) = \mu^{-(1+r\gamma)\delta\frac{\kappa}{\nu}-2} \exp\left(-\frac{\delta\kappa}{\nu r}\right).$$

5.2. Presentation of the numerical scheme. We use a discretization based on the reformulation (34). It is inspired by [8] and is fairly close to the so-called Chang-Cooper scheme [16].

We use a finite-volume scheme. The rectangle Ω_b is discretized with a structured regular mesh of size Δr and $\Delta\mu$ in each respective direction. The centers of the control volumes are the points (r_i, μ_j) with $r_i = \Delta r/2 + i\Delta r$ and $\mu_j = \Delta\mu/2 + j\Delta\mu$ for $i \in \{0, \dots, N_r - 1\}$ and $j \in \{0, \dots, N_\mu - 1\}$. We also introduce the intermediate points $r_{i+1/2}$ with $i \in \{-1, \dots, N_r - 1\}$ and $\mu_{j+1/2}$ with $j \in \{-1, \dots, N_\mu - 1\}$ defined with the same formula as before. The approximation of the solution on the cell (i, j) is denoted by

$$f_{ij} \approx \frac{1}{\Delta r \Delta \mu} \int_{r_{i-1/2}}^{r_{i+1/2}} \int_{\mu_{j-1/2}}^{\mu_{j+1/2}} f^{\text{ad}}(r, \mu) \, dr \, d\mu.$$

The scheme reads, for all $i \in \{0, \dots, N_r - 1\}$ and $j \in \{0, \dots, N_\mu - 1\}$,

$$(37) \quad \begin{cases} F_{i+1/2, j} - F_{i-1/2, j} + G_{i, j+1/2} - G_{i, j-1/2} = 0, \\ F_{N_r-1/2, j} = F_{-1/2, j} = G_{i, N_\mu-1/2} = G_{i, -1/2} = 0 \\ \sum_{i, j} f_{ij} \Delta r \Delta \mu = 1 \end{cases}$$

where the fluxes are given by a centered discretization of the reformulation (34), namely

$$(38) \quad F_{i+1/2, j} = -\frac{\Delta\mu}{\Delta r} r_{i+1/2}^2 \left(\frac{h^{(1)}(r_{i+1/2}, \mu_j)}{h^{(1)}(r_{i+1}, \mu_j)} f_{i+1, j} - \frac{h^{(1)}(r_{i+1/2}, \mu_j)}{h^{(1)}(r_i, \mu_j)} f_{ij} \right),$$

and

$$(39) \quad G_{i, j+1/2} = -\nu \frac{\Delta r}{\Delta \mu} \mu_{j+1/2}^2 \left(\frac{h^{(2)}(r_i, \mu_{j+1/2})}{h^{(2)}(r_i, \mu_{j+1})} f_{i, j+1} - \frac{h^{(2)}(r_i, \mu_{j+1/2})}{h^{(2)}(r_i, \mu_j)} f_{ij} \right).$$

One can show that the scheme (37) possesses a unique solution which is non-negative by following, for instance, the arguments of [15, Proposition 3.1]. Moreover, by construction, the scheme is exact in the case $\gamma = 0$.

Remark 5.1 (Choice of r_{\min} , r_{\max} , μ_{\min} , μ_{\max}). *Clearly f decays faster at infinity than ρ_0 since the convection term coming from the binding phenomenon brings mass closer to the origin. Therefore an appropriate choice for r_{\max} and μ_{\max} , coming from the decay of the involved inverse gamma distributions, should be (say)*

$r_{\max}^{-\delta} \leq 10^{-8}$ and $\mu_{\max}^{-\delta\kappa/\nu} \leq 10^{-8}$ so that the error coming from the tails of the distributions in the computation of moments is negligible. Similarly, near the origin the distributions decay very quickly to 0 (as $\exp(-1/\cdot)$). Therefore μ_{\min} , r_{\min} can be taken not too small without influencing the precision in the computation of moments of the solution. In practice, we chose $\mu_{\min} = r_{\min} = 0.06$. Observe that even if nothing prevents the choice $\mu_{\min} = r_{\min} = 0$ on paper, one experiences in practice a bad conditioning of the matrix which has to be inverted for solving the scheme.

Remark 5.2 (Implementation). Observe that the matrix which has to be inverted in order to solve the scheme is not a square matrix because of the mass constraint (which is necessary to ensure uniqueness of the solution). In practice, in order to solve the corresponding linear system $MF = B$ where $F = (f_{ij})_{ij}$ and $B = (0, \dots, 0, 1) \in \mathbb{R}^{N_r N_\mu + 1}$ and $M \in \mathbb{R}^{(N_r N_\mu + 1) \times N_r N_\mu}$ we use the pseudo-inverse yielding $F = (M^t M)^{-1} M^t B$. Finally the use of a sparse matrix routine greatly improves the computation time. Our implementation was made using Matlab. The code is publicly available on GitLab [17].

5.3. Numerical results. In our test cases we use the following parameters: $r_{\min} = 0.06$, $r_{\max} = 5$, $\mu_{\min} = 0.05$, $\mu_{\max} = 5$, $\delta = 8$, $N_r = 70$, $N_\mu = 200$, $\kappa = 1$, $\nu = 1$.

On Figure 3 we compare the distribution functions $f(r, \mu)$ obtained for various sets of parameters (p, γ) . We also draw the corresponding marginal $\rho(r)$ as well as ρ_0 and ρ_{fast} . We observe that for small values of p , ρ_{fast} is a good approximation of ρ . For larger values it tends to amplify the phenomenon of variance reduction.

In order to confirm that the main Fokker-Planck model reduces the coefficient of variation as soon as $\gamma > 0$ we draw on Figure 4 the coefficient of variation for each distribution ρ, ρ_{fast} relatively to that of ρ_0 for several values of p . We observe that indeed, the coefficient of variation is reduced. As in the case of fast μ RNA, the decay is more pronounced when the production of μ RNA is higher than that of mRNA, namely when $p > 1$. Interestingly enough, one also notices that the approximation ρ_{fast} increases the reduction of CV when $p > 1$ and diminishes it when $p < 1$. A transition at the special value $p = 1$ was already observed on Figure 1.

6. COMMENTS ON THE CHOICE OF NOISE

In this section, we discuss the influence of the type of noise in the Fokker-Planck models. Let us go back to the system of stochastic differential equations considered at the beginning and generalize it as follows

$$\begin{cases} dr_t &= (c_r - c r_t \mu_t - k_r r_t) dt + \sqrt{2\sigma_r D(r_t)} dB_t^1, \\ d\mu_t &= (c_\mu - c r_t \mu_t - k_\mu \mu_t) dt + \sqrt{2\sigma_\mu D(\mu_t)} dB_t^2, \end{cases}$$

with D some given function. In the models of the previous sections we chose $D(x) = x^2$. On the one hand it is natural to impose that $D(x)$ vanishes when $x \rightarrow 0$ in order to preserve the non-negativity of r_t and μ_t . On the other hand it is clear that the growth at infinity influences the tail of the equilibrium distribution which solves the corresponding Fokker-Planck equation. With a quadratic D we obtained algebraically decaying distributions. Nevertheless one may wonder if the decay of cell to cell variation due to μ RNA would still be observed if D is changed so that it involves distributions with faster decay at infinity. In order to answer this question, we choose a simple enough function D so that we can still derive analytical formulas for distributions of mRNA without binding and mRNA in the presence of “fast” μ RNA. Let us assume that

$$D(r) = r.$$

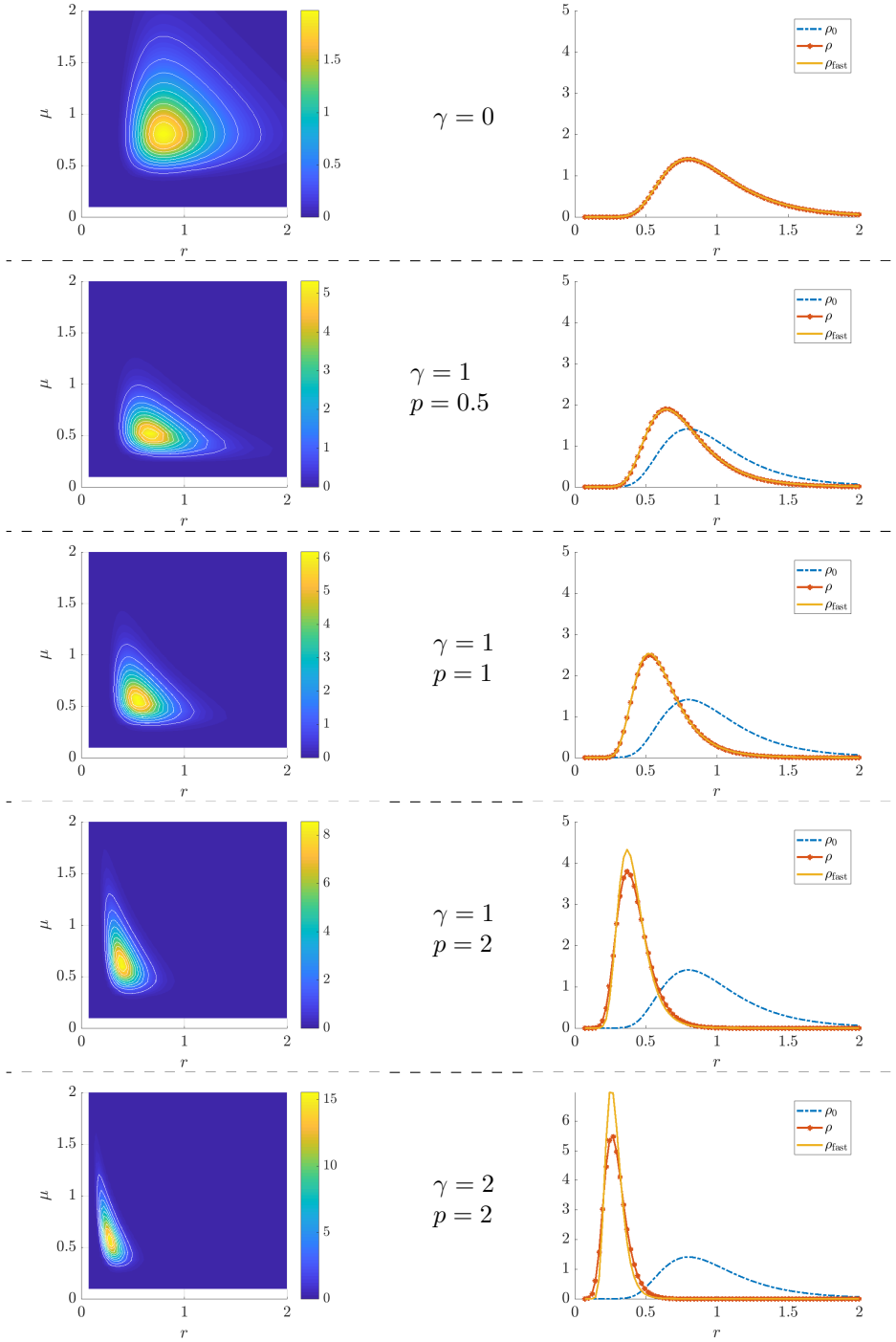


FIGURE 3. **Numerical results.** Numerical solution of the main Fokker-Planck model for various sets of parameters (γ, p) . *Left:* Surface and contour plot of the distribution function $f(r, \mu)$. The truncation at $r = 2$ and $\mu = 2$ is only for visualization purposes. *Right:* Corresponding marginal density ρ compared with ρ_{fast} and ρ_0 .

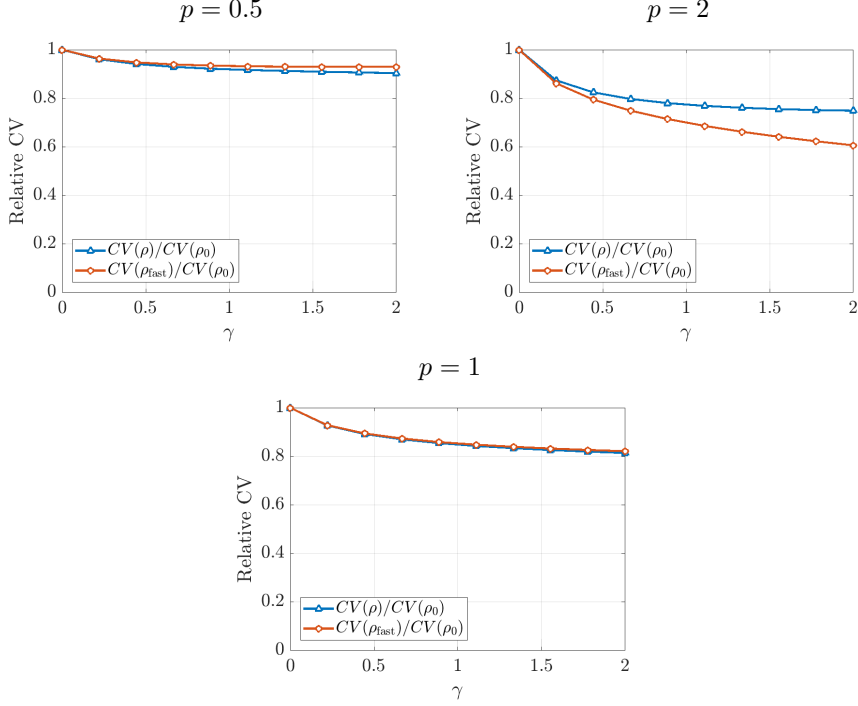


FIGURE 4. **Numerical results.** Relative coefficient of variation versus γ for various values of p .

6.1. Explicit formulas for distribution of mRNAs. In terms of modeling we may argue as in Section 2 and Section 3 in order to introduce the stationary probability distribution of mRNA without binding $\tilde{\rho}_0$ which solves

$$\partial_r [\sigma_r \partial_r (r \tilde{\rho}_0) - (c_r - k_r r) \tilde{\rho}_0] = 0.$$

It may still be solved analytically and one finds a gamma distribution

$$(40) \quad \tilde{\rho}_0(r) = \gamma_{\frac{c_r}{\sigma_r}, \frac{k_r}{\sigma_r}}(r) = C_{\frac{c_r}{\sigma_r}, \frac{k_r}{\sigma_r}} r^{\frac{c_r}{\sigma_r} - 1} e^{-\frac{k_r}{\sigma_r} r}$$

instead of an inverse gamma distribution in the quadratic case. The normalization constant is given in Section 3.1.

In the case of fast μ RNA, we may once again follow the method of Section 2 and Section 3 and introduce $\tilde{\rho}_{\text{fast}}$ solving

$$\partial_r [\partial_r (\sigma_r r \tilde{\rho}_{\text{fast}}) - (c_r - c r \tilde{j}_{\text{fast}}(r) - k_r r) \tilde{\rho}_{\text{fast}}] = 0$$

where the conditional expectation of the number of μ RNA within the population with r mRNA is given by

$$\tilde{j}_{\text{fast}}(r) = \int_0^\infty \mu \gamma_{\frac{c_\mu}{\sigma_\mu}, \frac{k_\mu + c r}{\sigma_\mu}}(\mu) d\mu = \frac{c_\mu}{k_\mu + c r}.$$

A direct computation then yields

$$(41) \quad \tilde{\rho}_{\text{fast}}(r) = C \left(1 + \frac{c}{k_\mu} r\right)^{-\frac{c_\mu}{\sigma_r}} r^{\frac{c_r}{\sigma_r} - 1} e^{-\frac{k_r}{\sigma_r} r},$$

with $C \equiv C(c_r, c_\mu, c, k_r, k_\mu, \sigma_r, \sigma_\mu)$ a normalizing constant.

Remark 6.1. Observe that the conditional expectation of the number of μ RNA within the population with r mRNA is unchanged, namely $\tilde{j}_{\text{fast}}(r) = j_{\text{fast}}(r)$. More generally, the expectation of a univariate process $(X_t)_t$ satisfying an SDE with linear

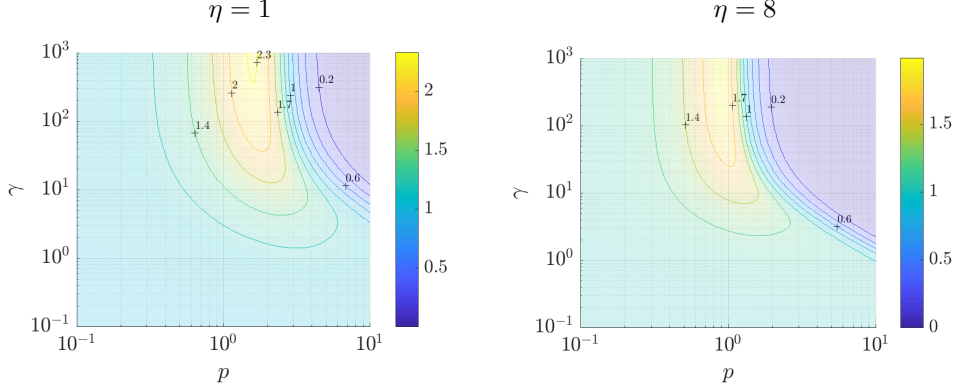


FIGURE 5. Numerical computation of the cell to cell variation. Relative cell to cell variation $CV(\tilde{\rho}_{fast}^{\eta,\gamma,p})/CV(\rho_0^\eta)$ for various parameters p , γ and η . On the horizontal axis, left means more production of mRNA and right means more production of μ RNA; On the vertical axis, top means more destruction of mRNA by binding and bottom means more destruction/consumption of mRNA by other mechanisms.

drift $dX_t = (a + bX_t) dt + \sqrt{2\sigma(X_t)} dB_t$ does not depend on the diffusion coefficient σ as its density g satisfy $\partial_t g(t, x) + \partial_x((a + bx)g(t, x)) - \partial_{xx}^2(\sigma(x)g(t, x)) = 0$, so that multiplying by x and integrating yields $dE[X_t] = (a + bE[X_t]) dt$ on its expectation $E[X_t]$. The argument also holds for multivariate processes.

6.2. Dimensional analysis. Once again we seek the parameters of importance among the many parameters of the model by a dimensional analysis. The characteristic value of r remains $\bar{r} = c_r/k_r$ as it is the expectation of $\tilde{\rho}_0$. After rescaling we find the new distribution

$$(42) \quad \tilde{\rho}_0^\eta(r) = \gamma_{\eta,\eta}(r) = C_{\eta,\eta} r^{\eta-1} e^{-\eta r},$$

and

$$(43) \quad \tilde{\rho}_{fast}^{\eta,\gamma,p}(r) = C_{fast}^{ad} \frac{r^{\eta-1}}{(1 + \gamma r)^{p\eta}} e^{-\eta r}.$$

where the parameters p and γ are given by (27) and (26) respectively and still quantify the intensity of the binding and the respective production of μ RNA versus mRNA. The new parameter η is given by

$$(44) \quad \eta = \frac{c_r}{\sigma_r}.$$

In the context of a dimensional analysis, let us mention that it would be inaccurate to compare η and δ as the σ_r (and σ_μ) do not represent the same quantity depending on the choice of D . For $D(r) = r^2$ it has the same dimension as k_r so $\delta = k_r/\sigma_r$ is the right dimensionless parameter. Here it has the same dimension as c_r , which justifies the introduction of η .

6.3. Numerical computation of the cell to cell variation. The expectation, variance and coefficient of variation of $\tilde{\rho}_0$ are explicitly given by

$$(45) \quad \text{Exp}(\tilde{\rho}_0^\eta) = 1, \quad \text{Var}(\tilde{\rho}_0^\eta) = \frac{1}{\eta}, \quad \text{CV}(\tilde{\rho}_0^\eta) = \frac{1}{\sqrt{\eta}},$$

As there is no explicit formula for the coefficient of variation of $\tilde{\rho}_{fast}^{\eta,\gamma,p}$ we evaluate it numerically as in Section 4.3. The results are displayed on Figure 5. We

observe that unlike the case of a quadratic diffusion coefficient the relative cell to cell variation, *i.e.* the cell to cell variation in the presence of μ RNA relative to cell to cell variations of the free case, is not unconditionally less than 1. For a large enough production of μ RNA, it eventually decays when the binding effect is very strong. However for smaller production of μ RNA or when the binding is weak, the effect is the opposite as the relative cell to cell variation is greater than 1. This is not satisfactory from the modeling point of view.

In conclusion the choice of noise is important in this model. An unconditional cell to cell variation decay in the presence of μ RNA is observed for quadratic noise only. While other choices of noise may still lead to similar qualitative results, the choice $D(r) = r^2$ allowed us to derive explicit formulas for the approximate density ρ_{fast} which, as numerical simulations show, is fairly close to the marginal ρ corresponding to the solution of the main Fokker-Planck model.

7. CONCLUDING REMARKS AND PERSPECTIVES

In this paper, we introduced a new model describing the joint probability density of the number of mRNA and μ RNA in a cell. It is based on a Fokker-Planck equation arising from a system of chemical kinetic equations for the number of two RNAs. The purpose of this simple model was to provide a mathematical framework to investigate how robustness in gene expression in a cell is affected by the presence of a regulatory feed-forward loop due to production of μ RNAs which bind to and deactivate mRNAs.

Thanks to the combined use of analytical formulas and numerical simulations, we showed that robustness of gene expression is indeed affected by the presence of a feed-forward loop involving μ RNA production. However, whether the effect is regulatory or de-regulatory strongly depends on the assumptions made on the type of noise affecting both mRNA and μ RNAs production. In the case of geometric noise (the diffusivity being quadratic in the solution itself), the effect is to reduce the spread of the distribution as the reduction of the coefficient of variation shows. In the case of sub-geometric noise (the diffusivity being only linear in the solution itself), the effect increases the spread as shown by the increase of the coefficient of variation. We may attempt an explanation by comparing the mRNA distribution in the absence of μ RNA and in the limit of fast μ RNA in the two cases. In the quadratic diffusivity case, both distributions are fat-tailed (*i.e.* they decay polynomially with the number of unbound mRNA molecules r , see (13) and (16)) but the rate of decay at infinity is modified by the presence of μ RNAs. On the other hand, in the linear diffusivity case, both decay exponentially fast (see (40) and (41)) and the exponential rate of decay is the same with or without μ RNAs. We propose that this might be the reason of the difference: in the quadratic diffusivity case, the change in polynomial decay allows to greatly reduce the standard deviation without affecting too much the mean, which results in a reduction of the coefficient of variation. In the linear diffusivity case, the exponential tail is not modified, which implies that the core of the distribution must be globally translated towards the origin, which affects the mean and the standard deviation in a similar way and does not systematically reduce the coefficient of variation. Which type of noise corresponds to the actual data is unknown at this stage. While quadratic diffusivity seems a fairly reasonable assumption (it is used in a number of contexts such as finance), it would require further experimental investigations to be fully justified in the present context. This discussion shows that the effect of μ RNA on noise regulation of mRNA translation is subtle and not easily predictable.

Along the way we provided theoretical tools for the analysis of the Fokker Planck equation at play and robust numerical methods for simulations. As the main biological hypothesis for the usefulness of μ RNA in the regulation of gene expression is based on their ability to reduce external noise, we also discussed the particular choice of stochasticity in the model.

There are several perspectives to this work. A first one would be the calibration of the parameters of the model from real-world data. This would allow to quantify more precisely the amount of cell-to-cell variation reduction due to μ RNA, thanks to the thorough numerical investigation done in this contribution of the effects of the parameters of the model. Besides, another perspective would be an improvement of Inequality (32) to the Conjecture (4.3). This would bring a definitive theoretical answer to the hypothesis of increased gene expression level in the simplified model of “fast” μ RNAs. One may also look into establishing a similar inequality for the general model. Finally, the gene regulatory network in a cell is considerably more complex than the simple, yet enlightening in our opinion, dynamics proposed in this paper. A natural improvement would be the consideration of more effects in the model, such as the production of the transcription factor, or the translation of mRNA into proteins, among many others.

APPENDIX A. COMPLEMENTARY RESULTS

A.1. Poincaré inequalities for gamma and inverse gamma distributions.

In this section we give a elementary proof of the 1D version of the Brascamp and Lieb inequality (see [14, Theorem 4.1], [11]), which is an extension of the Gaussian Poincaré inequality in the case of log-concave measures. This allows us to derive a weighted Poincaré inequality for the gamma distribution and deduce, by a change of variable, a similar functional inequality for the inverse gamma distribution.

Proposition A.1. *Let $I \subset \mathbb{R}$ be an open non-empty interval and $V : I \rightarrow \mathbb{R}$ a function of class \mathcal{C}^2 . Assume that*

- (i) V is strictly convex;
- (ii) e^{-V} is a probability density on I ;
- (iii) V tends to $+\infty$ at the extremities of I .

Then, for any suitably integrable function u , one has

$$(46) \quad \int_I |u(x) - \langle u \rangle_{e^{-V}}|^2 e^{-V(x)} dx \leq \int_I |u'(x)|^2 e^{-V(x)} (V''(x))^{-1} dx,$$

where for a density ν the notation $\langle u \rangle_\nu$ denotes $\int u \nu$.

Proof. Without loss of generality, as one may replace u with $u - \langle u \rangle_{e^{-V}}$, we assume that $\langle u \rangle_{e^{-V}} = 0$. We also assume that u is of class \mathcal{C}^1 and compactly supported in I and one can then extend *a posteriori* the class of admissible function by a standard density argument. Then, using (ii) one has

$$\begin{aligned} \int_I |u(x)|^2 e^{-V(x)} dx &= \frac{1}{2} \iint_{I \times I} |u(x) - u(y)|^2 e^{-(V(x)+V(y))} dx dy \\ &= \frac{1}{2} \iint_{I \times I} \left| \int_x^y u'(z) dz \right|^2 e^{-(V(x)+V(y))} dx dy. \end{aligned}$$

Now using the Cauchy-Schwarz inequality and assumption (i) one has

$$\begin{aligned} \int_I |u(x)|^2 e^{-V(x)} dx &\leq \\ &\frac{1}{2} \iint_{I \times I} \left(\int_x^y |u'(z)|^2 (V''(z))^{-1} dz \right) \left(\int_x^y V''(z) dz \right) e^{-(V(x)+V(y))} dx dy. \end{aligned}$$

Then take any point $x_0 \in I$ and define

$$U(x) = \int_{x_0}^x |u'(z)|^2 (V''(z))^{-1} dz,$$

so that the inequality rewrites

$$\begin{aligned} & \int_I |u(x)|^2 e^{-V(x)} dx \\ & \leq \frac{1}{2} \iint_{I \times I} (U(y) - U(x)) (V'(y) - V'(x)) e^{-(V(x)+V(y))} dx dy. \end{aligned}$$

Now just expand the right-hand side and use Fubini's theorem on each term as well as assumptions (ii) and (iii) to obtain

$$\int_I |u(x)|^2 e^{-V(x)} dx \leq \int_I U(x) V'(x) e^{-V(x)} dx.$$

One concludes by integrating the right-hand side by parts and observing that boundary terms vanish again by assumption (iii). \square

Remark A.2. *The proof is an adaptation of the original proof of the (flat) Poincaré-Wirtinger inequality by Poincaré.*

Observe that for $I = \mathbb{R}$ and $V(x) = x^2/2$, one recovers the classical Gaussian Poincaré inequality.

Remark A.3. *The inequality is sharp. It is an equality for functions of the form $u(x) = aV'(x) + b$, with $a, b \in \mathbb{R}$ if V is such that $V'(x)e^{-V(x)}$ tends to 0 at the boundaries, and only for constant functions otherwise (i.e. $a = 0$ and $b \in \mathbb{R}$).*

From the Brascamp-Lieb inequality, we now infer Poincaré inequalities for gamma and inverse gamma distributions.

Proposition A.4. *Let $\alpha > 1$ and $\beta > 0$. Then, for any functions u, v such that the integrals make sense, one has*

$$(47) \quad \int_0^\infty |u(x) - \langle u \rangle_{\gamma_{\alpha,\beta}}|^2 \gamma_{\alpha,\beta}(x) dx \leq \frac{1}{\alpha - 1} \int_0^\infty |u'(x)|^2 \gamma_{\alpha,\beta}(x) x^2 dx,$$

and

$$(48) \quad \int_0^\infty |v(y) - \langle v \rangle_{g_{\alpha,\beta}}|^2 g_{\alpha,\beta}(y) dy \leq \frac{1}{\alpha - 1} \int_0^\infty |v'(y)|^2 g_{\alpha,\beta}(y) y^2 dy,$$

where for a probability density ν the notation $\langle u \rangle_\nu$ denotes $\int u \nu$.

Proof. The first inequality is an application of (46) with $V(x) = \beta x - (\alpha - 1) \ln(x) - \ln(C_{\alpha,\beta})$, where $C_{\alpha,\beta} = \beta^\alpha / \Gamma(\alpha)$. Then take $v(y) = u(1/y)$ and make the change of variable $y = 1/x$ in all the integrals of (47) to get the result. \square

Remark A.5. *To the best of our knowledge the classical Bakry and Emery method does not seem to apply to show directly the functional inequalities of Proposition A.4. Let us give some details. In order to show a Poincaré inequality of the type*

$$\int_I |u(x) - \langle u \rangle_{e^{-V}}|^2 e^{-V(x)} dx \leq \int_I |u'(x)|^2 e^{-V(x)} D(x) dx,$$

for V as in Proposition A.1, it is sufficient that D and V satisfy the following curvature-dimension inequality

$$(49) \quad R(x) := \frac{1}{4}(D'(x))^2 - \frac{1}{2}D''(x)D(x) + D(x)^2V''(x) + \frac{1}{2}D'(x)D(x)V'(x) \geq \lambda_1 D(x),$$

for some positive constant $\lambda_1 > 0$. We refer to [5, 6] for the general form of the latter Bakry-Emery condition (for multidimensional anisotropic inhomogeneous diffusions) and to [2] or [1] for the simpler expression in the case of isotropic inhomogeneous diffusion, as discussed here. In the case of the inequalities (47) and (48), one has respectively $D(x) = x^2/(\alpha - 1)$, $V(x) = \beta x - (\alpha - 1) \ln(x) - \ln(C_{\alpha,\beta})$ and $D(y) = y^2/(\alpha - 1)$, $V(y) = \beta/y + (\alpha + 1) \ln(y) - \ln(C_{\alpha,\beta})$, which yields respectively $R(x) = \beta x^3/(\alpha - 1)^2$ and $R(y) = \beta y/(\alpha - 1)^2$. As claimed above, neither (47) nor (48) satisfy the condition (49). One also observes that in both cases the curvature-dimension inequality fails because of a degeneracy at one end of the interval.

Let us finally mention that there are in the literature other occurrences of Poincaré and more generally convex Sobolev inequalities for gamma distributions [4, 28, 7, 3]. However, we found out that the diffusion coefficient is always taken of the form $D(x) = 4x/\beta$. This weight, associated with the gamma invariant measure, corresponds to the Laguerre diffusion $L_{\alpha,\beta} f(x) = \beta x f''(\beta x) - (\alpha - \beta x) f'(\beta x)$. This operator differs from the adjoint of the one appearing in our model (6). In this case, one can check that the curvature-dimension condition of Bakry and Emery is satisfied as soon as $\alpha \geq 1/2$.

A.2. An upper bound for the relative cell to cell variation.

Proposition A.6. *One has the bound*

$$\text{CV}(\rho_{fast}^{\delta,\gamma,p}) \leq C_\delta := \left(\left(\frac{\delta}{\delta - 1} \right)^2 \left(1 - \frac{1}{(\delta - 1)^2} \right)^{\delta - 2} - 1 \right)^{\frac{1}{2}},$$

which holds for all $\delta > 2$, $\gamma > 0$ and $p \geq 0$.

Proof. The bound is a consequence of the Prékopa-Leindler inequality (see [14] and references therein) which states that if $f, g, h : \mathbb{R}^d \rightarrow [0, +\infty)$ are three functions satisfying for some $\lambda \in (0, 1)$ and for all x, y ,

$$(50) \quad h((1 - \lambda)x + \lambda y) \geq f(x)^{1-\lambda} g(y)^\lambda,$$

then

$$(51) \quad \|h\|_{L^1(\mathbb{R}^d)} \geq \|f\|_{L^1(\mathbb{R}^d)}^{1-\lambda} \|g\|_{L^1(\mathbb{R}^d)}^\lambda.$$

We use it with $\lambda = 1/2$, $f(x) = (1 + x)^{\gamma p \delta} x^{\delta - 2} e^{-\delta \gamma x}$ if $x \geq 0$ and $f(x) = 0$ if $x < 0$, $g(x) = x^2 f(x)$ and $h(x) = (1 + C_\delta^2)^{1/2} x f(x)$. The condition (50) is then equivalent to

$$(1 + C_\delta^2)^{-1/2} \leq \left[\frac{(1 + \frac{x+y}{2})}{(1+x)(1+y)} \right]^{\frac{\gamma p \delta}{2}} \left(\frac{y}{x} \right)^{\frac{1}{2}} \left(\frac{(\frac{y}{x})^{\frac{1}{2}} + (\frac{x}{y})^{\frac{1}{2}}}{2} \right)^{\delta - 1}$$

which is satisfied as the term between brackets is always greater than 1 and the function $z \mapsto z[(z + z^{-1})/2]^{\delta - 1}$, $z > 0$ is bounded from below by $(1 + C_\delta^2)^{-1/2}$, where C_δ is given in (32). Then with the change of variable $x' = 1/(\gamma x)$ in the integrals of (51), one recovers (32). \square

Acknowledgements

PD acknowledges support by the Engineering and Physical Sciences Research Council (EPSRC) under grants no. EP/M006883/1 and EP/N014529/1, by the Royal Society and the Wolfson Foundation through a Royal Society Wolfson Research Merit Award no. WM130048 and by the National Science Foundation (NSF) under grant no. RNMS11-07444 (KI-Net). PD is on leave from CNRS, Institut de Mathématiques de Toulouse, France. MH acknowledges support by the Labex CEMPI

(ANR-11-LABX-0007-01). SM acknowledges support by the CNRS–Royal Society exchange projects “CODYN” and “Segregation models in social sciences” and the Chaire Modélisation Mathématique et Biodiversité of Véolia Environment - École Polytechnique - Museum National d’Histoire Naturelle - Fondation X. All authors would like to thank Prof. Matthias Merckenshlager from Imperial College Institute of Clinical Sciences for bringing this problem to their attention and stimulating discussions.

Data statement

No new data were collected in the course of this research.

REFERENCES

- [1] Anton Arnold and Jean Dolbeault. Refined convex Sobolev inequalities. *J. Funct. Anal.*, 225(2):337–351, 2005.
- [2] Anton Arnold, Peter Markowich, Giuseppe Toscani, and Andreas Unterreiter. On convex Sobolev inequalities and the rate of convergence to equilibrium for Fokker-Planck type equations. *Comm. Partial Differential Equations*, 26(1-2):43–100, 2001.
- [3] Benjamin Arras and Yvik Swan. A stroll along the gamma. *Stochastic Process. Appl.*, 127(11):3661–3688, 2017.
- [4] D. Bakry. Remarques sur les semigroupes de Jacobi. *Astérisque*, (236):23–39, 1996. Hommage à P. A. Meyer et J. Neveu.
- [5] D. Bakry and Michel Émery. Diffusions hypercontractives. In *Séminaire de probabilités, XIX, 1983/84*, volume 1123 of *Lecture Notes in Math.*, pages 177–206. Springer, Berlin, 1985.
- [6] Dominique Bakry. L’hypercontractivité et son utilisation en théorie des semigroupes. In *Lectures on probability theory (Saint-Flour, 1992)*, volume 1581 of *Lecture Notes in Math.*, pages 1–114. Springer, Berlin, 1994.
- [7] Michel Benaïm and Raphaël Rossignol. Exponential concentration for first passage percolation through modified Poincaré inequalities. *Ann. Inst. Henri Poincaré Probab. Stat.*, 44(3):544–573, 2008.
- [8] Marianne Bessemoulin-Chatard, Maxime Herda, and Thomas Rey. Hypocoercivity and diffusion limit of a finite volume scheme for linear kinetic equations. *Math. Comp.*, 89(323):1093–1133, 2020.
- [9] Leonidas Bleris, Zhen Xie, David Glass, Asa Adadey, Eduardo Sontag, and Yaakov Benenson. Synthetic incoherent feedforward circuits show adaptation to the amount of their genetic template. *Molecular systems biology*, 7(1), 2011.
- [10] Rory Blevins, Ludovica Bruno, Thomas Carroll, James Elliott, Antoine Marcais, Christina Loh, Arnulf Hertweck, Azra Krek, Nikolaus Rajewsky, Chang-Zheng Chen, et al. micrnas regulate cell-to-cell variability of endogenous target gene expression in developing mouse thymocytes. *PLoS genetics*, 11(2), 2015.
- [11] S. G. Bobkov and M. Ledoux. From Brunn-Minkowski to Brascamp-Lieb and to logarithmic Sobolev inequalities. *Geom. Funct. Anal.*, 10(5):1028–1052, 2000.
- [12] Vladimir I. Bogachev, Nicolai V. Krylov, Michael Röckner, and Stanislav V. Shaposhnikov. *Fokker-Planck-Kolmogorov equations*, volume 207 of *Mathematical Surveys and Monographs*. American Mathematical Society, Providence, RI, 2015.
- [13] Carla Bosia, Matteo Osella, Mariama El Baroudi, Davide Corà, and Michele Caselle. Gene autoregulation via intronic micrnas and its functions. *BMC systems biology*, 6(1):131, 2012.
- [14] Herm Jan Brascamp and Elliott H. Lieb. On extensions of the Brunn-Minkowski and Prékopa-Leindler theorems, including inequalities for log concave functions, and with an application to the diffusion equation. *J. Functional Analysis*, 22(4):366–389, 1976.
- [15] Claire Chainais-Hillairet and Jérôme Droniou. Finite-volume schemes for noncoercive elliptic problems with Neumann boundary conditions. *IMA J. Numer. Anal.*, 31(1):61–85, 2011.
- [16] JS Chang and G Cooper. A practical difference scheme for Fokker-Planck equations. *Journal of Computational Physics*, 6(1):1–16, 1970.
- [17] Pierre Degond, Maxime Herda, and Sepideh Mirrahimi. FPMuRNA. <https://gitlab.inria.fr/herda/fpmurna>, 2020.
- [18] Pierre Degond, Shi Jin, and Yuhua Zhu. An uncertainty quantification approach to the study of gene expression robustness. *arXiv preprint arXiv:1910.07188*, 2019.
- [19] Margaret S Ebert and Phillip A Sharp. Roles for micrnas in conferring robustness to biological processes. *Cell*, 149(3):515–524, 2012.
- [20] David Gilbarg and Neil S. Trudinger. *Elliptic partial differential equations of second order*. Classics in Mathematics. Springer-Verlag, Berlin, 2001. Reprint of the 1998 edition.

- [21] Daniel T. Gillespie. A general method for numerically simulating the stochastic time evolution of coupled chemical reactions. *J. Comput. Phys.*, 22(4):403–434, 1976.
- [22] Daniel T Gillespie. The chemical langevin equation. *The Journal of Chemical Physics*, 113(1):297–306, 2000.
- [23] R. Z. Has'minskii. Ergodic properties of recurrent diffusion processes and stabilization of the solution of the Cauchy problem for parabolic equations. *Teor. Veroyatnost. i Primenen.*, 5:196–214, 1960.
- [24] Héctor Herranz and Stephen M Cohen. Micrnas and gene regulatory networks: managing the impact of noise in biological systems. *Genes & development*, 24(13):1339–1344, 2010.
- [25] Wen Huang, Min Ji, Zhenxin Liu, and Yingfei Yi. Integral identity and measure estimates for stationary Fokker-Planck equations. *Ann. Probab.*, 43(4):1712–1730, 2015.
- [26] Wen Huang, Min Ji, Zhenxin Liu, and Yingfei Yi. Steady states of Fokker-Planck equations: I. Existence. *J. Dynam. Differential Equations*, 27(3-4):721–742, 2015.
- [27] Per Lötstedt and Lars Ferm. Dimensional reduction of the Fokker-Planck equation for stochastic chemical reactions. *Multiscale Modeling & Simulation*, 5(2):593–614, 2006.
- [28] Laurent Miclo. Sur l'inégalité de Sobolev logarithmique des opérateurs de Laguerre à petit paramètre. In *Séminaire de Probabilités, XXXVI*, volume 1801 of *Lecture Notes in Math.*, pages 222–229. Springer, Berlin, 2003.
- [29] Frank W. J. Olver, Daniel W. Lozier, Ronald F. Boisvert, and Charles W. Clark, editors. *NIST handbook of mathematical functions*. U.S. Department of Commerce, National Institute of Standards and Technology, Washington, DC; Cambridge University Press, Cambridge, 2010. With 1 CD-ROM (Windows, Macintosh and UNIX).
- [30] Matteo Osella, Carla Bosia, Davide Corá, and Michele Caselle. The role of incoherent microrna-mediated feedforward loops in noise buffering. *PLoS Comput Biol*, 7(3):e1001101, 2011.
- [31] Benoît Perthame. *Parabolic equations in biology*. Lecture Notes on Mathematical Modelling in the Life Sciences. Springer, Cham, 2015. Growth, reaction, movement and diffusion.
- [32] N. G. van Kampen. *Stochastic processes in physics and chemistry*, volume 888 of *Lecture Notes in Mathematics*. North-Holland Publishing Co., Amsterdam-New York, 1981.

(P. Degond) DEPARTMENT OF MATHEMATICS, IMPERIAL COLLEGE LONDON, SOUTH KENSINGTON CAMPUS, LONDON, SW7 2AZ, UK

Email address: pdegond@imperial.ac.uk

(M. Herda) INRIA, UNIV. LILLE, CNRS, UMR 8524 – LABORATOIRE PAUL PAINLEVÉ, F-59000 LILLE, FRANCE.

Email address: maxime.herda@inria.fr

(S. Mirrahimi) INSTITUT DE MATHÉMATIQUES DE TOULOUSE, UMR 5219, UNIVERSITÉ DE TOULOUSE, CNRS, UPS IMT, F-31062 TOULOUSE CEDEX 9, FRANCE.

Email address: sepideh.mirrahimi@math.univ-toulouse.fr